Mixed salts of amino acids: Syntheses, crystal structure and vibrational spectra of L-histidinium(2+) · NO 3 · ClO 4 and L-histidinium....

Article *in* Zeitschrift für Kristallographie · September 2010

DOI: 10.1524/zkri.2010.1269

CITATIONS
8

READS
12

3 authors:

Aram Petrosyan
National Academy of Sciences of Armenia
118 PUBLICATIONS **1,249** CITATIONS
SEE PROFILE

Michel Fleck
University of Vienna
162 PUBLICATIONS **1,604** CITATIONS
SEE PROFILE

Vahram Ghazaryan
Institute of Applied Problems of Physics, Yere...
53 PUBLICATIONS **421** CITATIONS
SEE PROFILE

Z. Kristallogr. **225** (2010) 388–395 / **DOI** 10.1524/zkri.2010.1269

Mixed salts of amino acids: Syntheses, crystal structure and vibrational spectra of *L*-histidinium(2+) nitrate-perchlorate and *L*-histidinium(2+) nitrate-tetrafluoroborate

Aram M. Petrosyan[I], Michel Fleck*[,II] and Vahram V. Ghazaryan[I]

[I] Institute of Applied Problems of Physics, NAS of Armenia 25 Nersessyan Str., 0014 Yerevan, Armenia
[II] Institute of Mineralogy and Crystallography, University of Vienna, Althanstr. 14, 1090 Vienna, Austria

Received March 29, 2010; accepted July 5, 2010

Mixed salts / L-histidine nitrate-perchlorate / L-histidine nitrate-tetrafluoroborate / Single crystal structure analysis / X-ray diffraction / Vibrational spectra / Amino acid

Abstract. Crystals of *L*-histidinium(2+) nitrate-perchlorate (L-$His^{2+} \cdot NO_3^- \cdot ClO_4^-$) and *L*-histidinium(2+) nitrate-tetrafluoroborate (L-$His^{2+} \cdot NO_3^- \cdot BF_4^-$) have been obtained by crystallization from aqueous solutions. For both compounds, single-crystal XRD analysis as well as ATR FTIR and Raman spectroscopy was performed to determine and investigate the crystal structures, which turned out to be closely related, albeit not isotypic, although symmetry (space group $P2_12_12_1$, $Z = 4$) and unit cell parameters of both compounds match to some extent. In each case the asymmetric unit contains a doubly charged L-His^{2+} cation with the charge counterbalanced by NO_3^- as well as ClO_4^- or BF_4^- anions. The structural differences between both compounds are subtle, mainly expressed in different conformations of the *L*-histidinium(2+) cations, which leads to different hydrogen bond networks. The L-His^{2+} cations form O–H···O hydrogen bonds to the nitrate anions and weak N–H···O and N–H···F hydrogen bonds. Powder SHG tests confirm considerable second order nonlinear optical activity for L-$His^{2+} \cdot NO_3^- \cdot BF_4^-$ but not for L-$His^{2+} \cdot NO_3^- \cdot ClO_4^-$, this discrepancy being a result of the structural difference.

1. Introduction

Crystalline salts of optically active amino acids have been a subject of intensive research in recent years. This research has mainly focused on single salts [1, 2]. Formation mechanisms of single salts of *L*-arginine and *L*-histidine have been considered [3]. This is not the case for double salts or –more generally – salts with different cations and anions. Among minerals and inorganic compounds, such salts are widespread and comprehensively studied. The situation concerning mixed salts of amino acids is different: Similar studies are rare, although the importance of investigations of these compounds has been emphasized [3].

Among the examples of this group are double salts of potassium and ammonium with the glycinium cation ($K^+ \cdot Gly^+ \cdot SO_4^{2-}$, $NH_4^+ \cdot Gly^+ \cdot SO_4^{2-}$), [4–6] and ammonium with betainium ($(NH_4)^+ \cdot Bet^+ \cdot (SO_4)^{2-}$) [7]. However, there are numerous complex metal salts with different ligands (especially of copper (II)) with inorganic anion and a deprotonated amino acid as anion or even with different amino acids providing the anions. The authors of [8] patented a number of mixed fluorides-phosphates of *L*-lysine (*L*-Lys), *L*-hydroxylysine, *L*-ornithine (*L*-Orn), *L*-arginine (*L*-Arg) and *L*-histidine (*L*-His) because of their cariostatic properties. Regrettably, the authors did not provide any data confirming the structures of the compounds (IR spectra, XRD analysis) and therefore no unit cell data, let alone any determination of the structures. The first unambiguously established mixed salts of *L*-lysine, namely (L-$Lys^+ \cdot L$-Lys^{2+}) $\cdot$ 2 $Cl^- \cdot ClO_4^-$ and (L-$Lys^+ \cdot L$-Lys^{2+}) $\cdot$ 2 $Cl^- \cdot NO_3^-$ [9, 10] as well as *L*-ornithine ($2L$-$Orn^{2+} \cdot Cl^- \cdot NO_3^- \cdot SO_4^{2-}$) [11] were discovered by the group of R. K. Rajaram.

Recently, we pointed out that the preparation of mixed salts of amino acids can be considered as an approach for the discovery of new nonlinear optical materials among salts of amino acids [12]. Additionally, this research is interesting from both chemical and crystallochemical points of views, because it is not yet clear which amino acids can form mixed salts with which acids. Neither formation mechanisms nor structural features are in any way predictable. In this context it is worth noting that by using the term 'mixed salts' we do not mean solid solutions (see *e.g.* [13–15]), but compounds with definite composition and structure (although formation of solid solutions on their basis cannot be excluded).

Among the numerous studies on amino acid compounds, the discovery of nonlinear optical (NLO) properties of *L*-histidinium(+) tetrafluoroborate (L-$His \cdot HBF_4$) [16] attracted great interest to the salts of *L*-histidine as promising NLO materials. Consequently, many previously known as well as newly obtained salts of singly- and doubly-charged *L*-histidine cations (L-His^+ and L-His^{2+}, re-

* Correspondence author (e-mail: michel.fleck@univie.ac.at)

spectively) were studied – see the review [1] and references therein.

Previous work established that in the system *L*-His−HNO_3−H_2O the following species have been found: *L*-His · HNO_3, *L*-His · HNO_3 · H_2O, and *L*-His · 2 HNO_3 [17–20]. Investigation of the system *L*-His−HBF_4−H_2O proved that, in addition to the already known species *L*-His · HBF_4, two poorly crystallized polymorphs of *L*-His · 2 HBF_4 (α and β) with *L*-His^{2+} cation were obtained [1], while in the system *L*-His−$HClO_4$ – H_2O only the existence of the *L*-His · $HClO_4$ salt was established [21].

In the present paper we report the results of our study on the preparation, crystal structure determination and characterization by means of IR and Raman spectra of two novel *L*-histidinium(2+) double salts, viz. *L*-histidinium(2+) nitrate-perchlorate (*L*-$His^{2+} \cdot NO_3^- \cdot ClO_4^-$, compound I) and *L*-histidinium(2+) nitrate-tetrafluoroborate (*L*-$His^{2+} \cdot NO_3^- \cdot BF_4^-$, compound II).

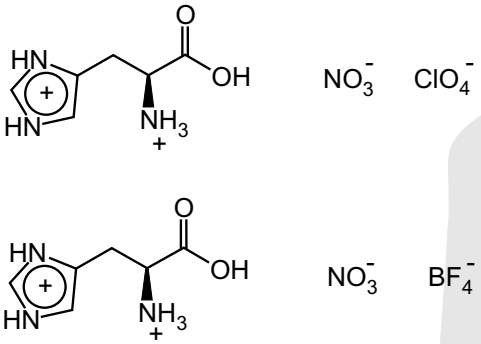

Schemes

2. Materials and methods

As initial reagents *L*-histidine purchased from Sigma Chem. Co., was used and "chem. pure" grade nitric, perchloric, and tetrafluoroboric acids, respectively. The title compounds were obtained by slow evaporation from aqueous solutions containing *L*-histidine, HNO_3 and $HClO_4$ or HBF_4, respectively, in 1 : 1 : 1 molar ratio at room temperature. Spontaneously formed crystals were colorless and of good quality (Figs. 1 and 2).

Single crystal X-ray intensity data were collected at 200 K on a Nonius APEX-II diffractometer with a CCD-area detector. The reflection data were processed with the Nonius program suite Bruker SMART, and corrected for Lorentz, polarization, background and absorption effects [22]. The crystal structures were determined by direct methods and subsequent Fourier and difference Fourier syntheses, followed by full-matrix least-squares refinements on F^2 [23]. All hydrogen atoms were refined freely in (II). In (I) some hydrogen atoms were treated as riding on their parent atoms. Using anisotropic treatment of the non-hydrogen atoms and unrestrained isotropic treatment of the hydrogen atoms, the refinements converged at *R* values of 0.033 and 0.049 for (I) and (II), respectively. Details of the measurements and crystallographic parameters are given in Table 1[1].

The attenuated total reflection Fourier transform infrared (ATR FTIR) spectra were registered using a Nicolet 5700 spectrophotometer fitted with a ZnSe prism (4000–650 cm^{-1}; number of scans: 64, resolution: 4 cm^{-1}), the part of spectra from 650–400 cm^{-1} were taken from the Nujol mull spectra measured on the same spectrophotometer (4000-400 cm^{-1}, number of scans: 32, resolution: 2 cm^{-1}). Fourier transform Raman spectra were registered using a NXP FT-Raman Module of the same spectrophotometer (number of scans: 256, laser power at sample: 0.3 W, resolution: 4 cm^{-1}).

Table 1. Crystal data and details of the refinement for (I) and (II).

	(I)	(II)
Formula	$C_6H_{11}ClN_4O_9$	$C_6H_{11}BF_4N_4O_5$
M_r	318.64	306.00
Crystal size, mm^3	0.06 × 0.06 × 0.09	0.02 × 0.04 × 0.05
Crystal system	Orthorhombic	Orthorhombic
Space group	$P2_12_12_1$	$P2_12_12_1$
a [Å]	6.7829(3)	7.430(2)
b [Å]	10.2466(3)	9.670(2)
c [Å]	17.1404(6)	17.072(3)
V [$Å^3$]	1191.29(8)	1226.9(5)
Z	4	4
D_{calcd} [g cm^{-3}]	1.777	1.656
μ (MoK_α) [cm^{-1}]	0.378	0.173
F(000)	656	624
Reflections measured	10669	8922
Reflections unique	3235	5249
Data with $F_o > 4\sigma(F_o)$	2946	4364
R_{int}	0.018	0.030
Parameters refined	208	226
$R(F)^a$ (for $F_o > 4\sigma(F_o)$)	0.033	0.049
$wR(F^2)^b$ (all reflections)	0.087	0.140
Weighting parameters *a*/*b*	0.042/0.324	0.074/0.161
Flack parameter [24]	0.01(5)	0.02(1)
$\Delta\varrho$ (max/min) [e $Å^{-3}$]	0.50/−0.26,	0.26/−0.36

a: $R_1 = \Sigma\,||F_o| - |F_c||/\Sigma\,|F_o|$,
b: $wR_2 = [\Sigma w(F_o^2 - F_c^2)^2/\Sigma wF_o^4]^{1/2}$, $w = 1/[\sigma^2(F_o^2) + (a \times P)^2 + b \times P]$, $P = (F_o^2 + 2F_c^2)/3$. *Note*: Scattering factors for neutral atoms were employed in the refinement.

3. Results and discussion

3.1 Possible formation mechanisms of mixed salts with different anions

On the basis of formation mechanisms of simple salts [3] and the two mechanisms described in [9–11], we have conceived fifteen possible combinations of mixed salts of amino acid cations with different anions [12]. More than

[1] Supplementary Material: Crystallographic data (excluding structure factors) for the structures reported in this paper have been deposited with the Cambridge Crystallographic Data Centre as supplementary publication no. 767417 (compound I) and 767418 (compound II). Copies of available material can be obtained, free of charge via www.ccdc.cam.ac.uk/data_request/cif, by emailing data_request@ccdc.cam.ac.uk, or by contacting The Cambridge Crystallographic Data Centre, 12, Union Road, Cambridge CB2 1EZ, UK; fax: +44 1223 336033.

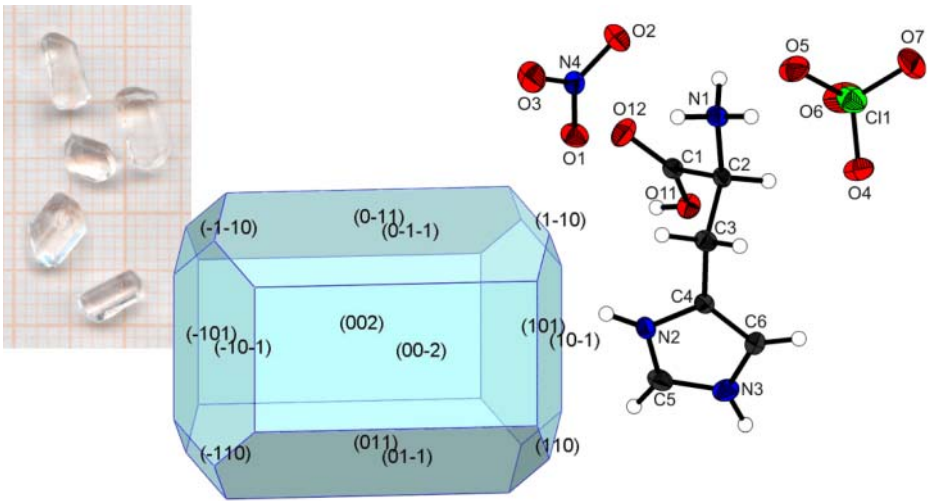

Fig. 1. Photograph of spontaneously formed crystals, crystal morphology and asymmetric part of unit cells of *L*-$His^{2+} \cdot NO_3^- \cdot ClO_4^-$ (I).

30 mixed salts of *L*-arginine, *L*-histidine, *L*-ornithine and *L*-lysine [12] were found as examples for these possible types. Both compounds presented in this paper belong to the $A^{2+} \cdot X(1)^- \cdot X(2)^-$ type.

3.2 Crystal and molecular structures of *L*-histidinium(2+) nitrate-perchlorate and *L*-histidinium(2+) nitrate-tetrafluoroborate

On a quick comparison of the crystal data, both species appear to be isostructural, at least when judging from their similar unit cell parameters and the same symmetry ($P2_12_12_1$). A closer inspection of the crystal structures reveals the following: both asymmetric units contain one doubly charged *L*-His^{2+} cation as well as one NO_3^- anion and one tetrahedral anion (BF_4^- or ClO_4^-, respectively). Since analogous compounds of perchlorates and tetrafluoroborates are usually isotypic, one might expect the same in this case. Nevertheless, the structures are not the same. Although the packing manner of both structures is similar, the conformations of the *L*-histidinium(2+) cations are different (Figs. 1 and 2), which in turn leads to different anion positions and, consequently, different hydrogen bond networks (Table 2).

One of the common features of both structures is the chemical state of the *L*-histidinium(2+) moieties: Both the α-amino group and the imidazole ring are protonated, while the carboxyl group is neutral, *i.e.* not deprotonated. This is reflected by the fact that the C=O- and C−O-bonds can be clearly distinguished via their lengths (C1=O12-distances of 1.202(2) Å in both compounds and C1−O11-distances of 1.318(2) Å and 1.311(2) Å in (I) and (II), respectively), both typical for the respective C=O and C−OH bond distances. These bond lengths agree very well with the respective values of those of *L*-His^{2+} in the structure of *L*-$His^{2+} \cdot 2\,NO_3^-$ [18, 19].

Hydroxyl groups usually form rather strong hydrogen bonds. As can be seen from Table 2, there are hydrogen bonds between the COOH groups and the nitrate anions in both compounds, with O···O distances of 2.617(2) Å and 2.583(2)Å in (I) and (II), respectively, which are similar to the respective O···O distance in the structure of *L*-His^{2+} $2NO_3^-$ (2.621 Å) [18, 19]. Likewise, the bond lengths and angles in the NO_3^- and the tetrahedral anions also correspond well to the respective values of nitrate [17–19], perchlorate [21] and tetrafluoroborate [26] anions reported previously. As evident from the O−N−O- and O−Cl−O- and F−B−F-angles (Table 3), the nitrate, perchlorate and tetrafluoroborate anions retain their usual configurations (planar and tetrahedral). The distance N4−O1 is significantly longer (1.268(4) and 1.264(2) Å) than the other two, which is probably due to the participation of the O1 atom in two hydrogen bonds (*i.e.* N2−H2N···O1 and the stronger O11−H1···O1). As can be seen from Table 2,

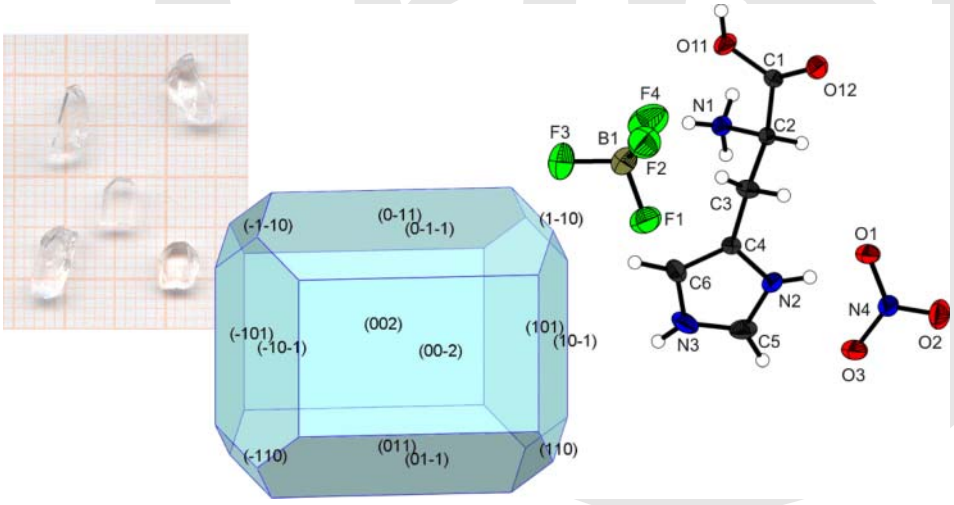

Fig. 2. Photograph of spontaneously formed crystals, crystal morphology and asymmetric part of unit cells of *L*-$His^{2+} \cdot NO_3^- \cdot BF_4^-$ (II).

Table 2. Hydrogen bond parameters (in Å and °) for (I) and (II). The selection of O−H···O, N−H···O and N−H···F contacts as hydrogen bonds was made based on [25].

L-$His^{2+} \cdot NO_3^- \cdot ClO_4^-$ (I)

D−H···A	*d*(D−H)	*d*(H···A)	*d*(D···A)	DHA
O11−H1···O1^{i}	0.80(3)	1.82(3)	2.617(2)	169(3)
N1−H11···O6^{ii}	0.89^{a}	2.31	3.063(2)	142
N1−H12···O2^{iii}	0.89^{a}	2.27	2.949(2)	133
N1−H13···O1	0.89^{a}	2.18	3.056(2)	167
N2−H2···O12^{iv}	0.84(3)	2.17(3)	2.890(2)	143(2)
N3−H3···O11^{v}	0.89(3)	2.40(3)	3.180(2)	148(2)

L-$His^{2+} \cdot NO_3^- \cdot BF_4^-$ (II)

D−H···A	*d*(D−H)	*d*(H···A)	*d*(D···A)	DHA
O11−H1···O1^{vi}	0.88(3)	1.72(3)	2.583(2)	165(3)
N1−H11···O12^{vi}	0.81(3)	2.11(3)	2.898(2)	163(2)
N1−H12···O3^{vii}	0.87(3)	2.17(3)	2.859(2)	136(2)
N1−H13···F3^{viii}	0.83(3)	2.11(4)	2.901(2)	161(4)
N2−H2···O1	0.84(3)	2.07(3)	2.899(2)	172(3)
N3−H3···F1^{ix}	0.80(3)	2.02(3)	2.823(2)	177(3)

a: N−H-distances constrained to 0.89 Å.
Symmetry code of A: (i) $x-{}^1/_2, -y+{}^3/_2, 2-z$; (ii) $-x, y+{}^1/_2, -z+{}^3/_2$; (iii) $2-x, y-{}^1/_2, -z+{}^3/_2$; (iv) $x+{}^1/_2, -y+{}^3/_2, -z+2$; (v) $x+{}^1/_2, -y+{}^1/_2, -z+2$; (vi) $1-x, y+{}^1/_2, -z+{}^1/_2$; (vii) $x+{}^1/_2, -y+{}^1/_2, -z$; (viii) $1-x, y-{}^1/_2, -z+{}^1/_2$; (ix) $x+{}^1/_2, -y+{}^3/_2, -z$.

the N−H···O type hydrogen bonds are generally very weak, the majority of them being on the level of van der Waals interactions. According to Zefirov [25], the intermediate H···O distance range of 2.15–2.45 Å (for O−H···O and N−H···O contacts) corresponds to the weakest hydrogen bonds and the strongest van der Waals interactions. Packing diagrams of compounds (I) and (II) are shown in Fig. 3.

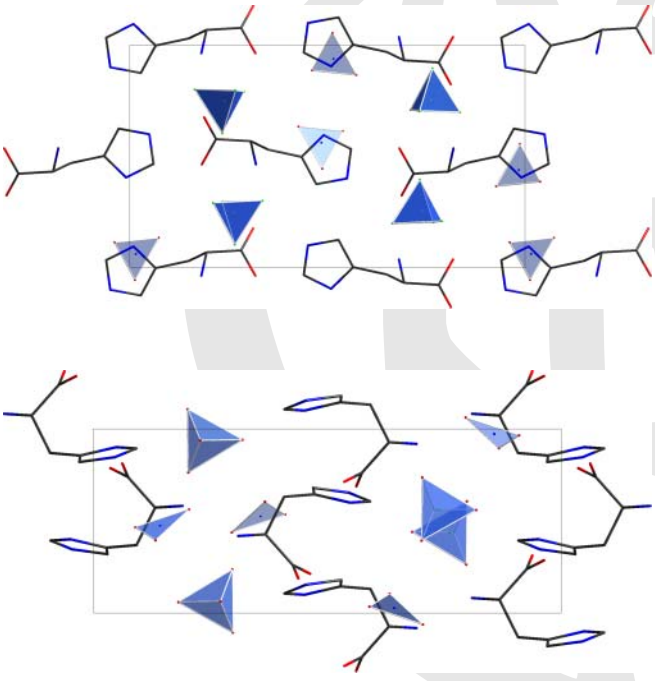

Fig. 3. Packing diagrams of (I) and (II). NO_3-groups displayed as triangles, BF_4- and ClO_4-groups as tetrahedra, respectively. Note the different conformations of the *L*-histidinium molecules.

In spite of all these similarities, the structures of (I) and (II) have some important discrepancies. Although the ClO_4^- anion is larger than its BF_4^- analogue (mean Cl−O distance 1.429 Å, mean B−F distance 1.389 Å), the unit cell volume is smaller for the perchlorate salt ($V = 1191.29(8)$ Å^3, in contrast to $V = 1226.9(5)$ Å^3 for the tetrafluoroborate salt). This difference can be explained by the different conformations of the *L*-histidinium(2+) cations: In (I), the carbon backbone of the *L*-

Table 3. Selected bond lengths (Å) and angles (°) for (I) and (II).

L-Histidinium molecules

Distance	(I)	(II)	Angle	(I)	(II)
C1−O11	1.318(2)	1.311(2)	O11−C1−O12	124.5(2)	125.2(1)
C1−O12	1.202(2)	1.202(2)	O11−C1−C2	112.8(1)	111.1(1)
C1−C2	1.519(2)	1.526(2)	O12−C1−C2	122.7(1)	123.7(1)
C2−N1	1.486(2)	1.487(2)	N1−C2−C1	108.2(1)	109.2(1)
C2−C3	1.542(2)	1.533(2)	N1−C2−C3	108.9(1)	111.2(1)
C3−C4	1.492(2)	1.495(2)	C1−C2−C3	111.9(1)	109.3(1)
C4−C6	1.352(2)	1.349(2)	C4−C3−C2	111.7(1)	113.9(1)
C6−N3	1.386(2)	1.369(2)	C6−C4−N2	105.8(1)	106.4(1)
N3−C5	1.315(2)	1.316(3)	C6−C4−C3	131.0(1)	129.5(1)
C5−N2	1.320(2)	1.329(2)	N2−C4−C3	122.9(1)	124.1(1)
N2−C4	1.381(2)	1.376(2)	N3−C5−N2	107.8(1)	107.7(1)
			C4−C6−N3	106.7(1)	106.9(2)
			C5−N2−C4	110.2(1)	109.2(1)
			C5−N3−C6	109.4(1)	109.7(1)

NO_3 groups

Distance	(I)	(II)	Angle	(I)	(II)
N4−O1	1.268(2)	1.264(2)	O1−N4−O2	118.4(1)	123.7(2)
N4−O2	1.241(2)	1.229(2)	O1−N4−O3	120.1(1)	117.6(1)
N4−O3	1.225(2)	1.231(2)	O2−N4−O3	121.5(2)	118.7(2)

Tetrahedral groups

Distance	(I)	(II)
Cl−O4/B−F1	1.444(1)	1.401(2)
Cl−O5/B−F2	1.431(1)	1.385(2)
Cl−O6/B−F3	1.424(2)	1.380(2)
Cl−O7/B−F4	1.416(2)	1.388(2)
Angle	**(I)**	**(II)**
F3−B1−F2/O7−Cl1−O6	110.9(2)	108.9(1)
F3−B1−F4/O7−Cl1−O5	110.9(2)	109.7(1)
F2−B1−F4/O6−Cl1−O5	107.3(1)	110.4(1)
F3−B1−F1/O7−Cl1−O4	109.0(1)	109.1(1)
F2−B1−F1/O6−Cl1−O4	108.5(1)	108.56(9)
F4−B1−F1/O5−Cl1−O4	110.2(1)	110.17(9)

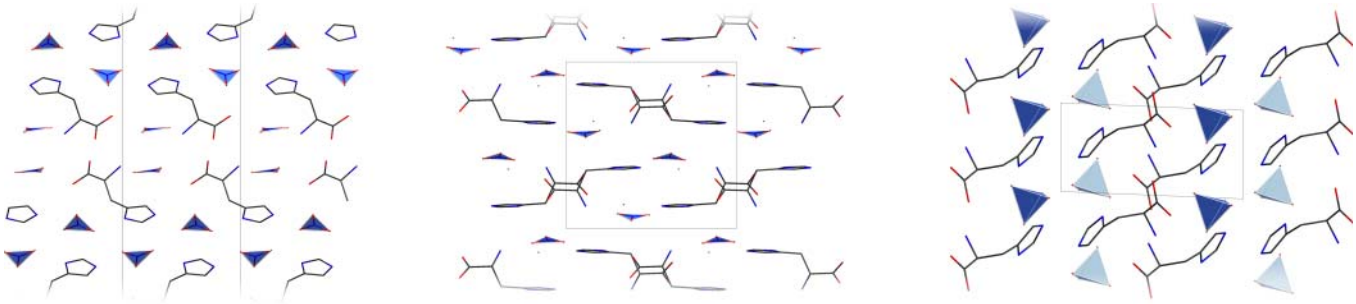

Fig. 4. Structure of (L-$His^{2+} \cdot 2\,NO_3^-$) viewed along [1 0 0] (left, [19]), (L-$His^+ \cdot NO_3^- \cdot H_2O$) viewed along [0 1 0] (middle, [17]), and (L-$His^{2+} \cdot 2BF_4^-$) viewed along [1 0 0] (right, [26]). Note that in all cases the conformations of the L-histidinium molecules are *trans*.

histidinium(2+) cation shows *gauche*-conformation (torsion angle C1−C2−C3−C4 of 55.8(2)°), in contrast to the nearly completely extended *trans*-conformation in (II) (torsion angle C1−C2−C3−C4 of 171.3(1)°). As expected, the C−C−C−N conformation is reciprocal, *i.e.* the N1−C2−C3−C4 torsion angles are 175.3(1)° and 50.7(2)°, respectively). This conformational distinction leads to a different network of hydrogen bonds. Generally, the hydrogen bonds in (II) are considerably stronger than those in (I), judged by the distances, as most of the hydrogen bonds, except one (O−H···O), are at the level of van der Waals interactions. The intramolecular bond lengths and angles are listed in Table 3.

There are several structural similarities between the title compounds and those of L-histidine nitrates [17], especially L-histidine dinitrate [18, 19], and L-histidine perchlorate [21]. The structure of L-histidine dinitrate (L-$His^{2+} \cdot 2NO_3^-$) is characterized by one L-histidinium(2+) cation, connected to two crystallographically different NO_3^- anions via an extensive hydrogen bond network. As in (II), the L-histidinium(2+) cation has *trans*-conformation (torsion angle C1−C2−C3−C4 of −179°), and the geometry of the whole molecule is similar to that in (II) (Fig. 4a). The compound crystallizes in the same orthorhombic space group as the title compounds, namely $P2_12_12_1$. This is also the case for L-histidinium(+) nitrate monohydrate (L-$His^+ \cdot NO_3^- \cdot H_2O$) [17], in which there is one moiety each in the asymmetric unit, the L-histidinium(+) moiety also extended to *trans*-conformation (torsion angle C1−C2−C3−C4 of −172.2(2)°, Fig. 4b). The same applies to L-histidinium(+) perchlorate (L-$His^+ \cdot ClO_4^-$) [21], the torsion angle C1−C2−C3−C4 being 176.8(2)°). This species has monoclinic symmetry ($P2_1$, Fig. 4c).

Most interestingly, the title compounds differ also in respect of their nonlinear optical activity. Preliminary assessment of their nonlinear optical activity, employing powder SHG tests, showed that (II) gives a relatively strong second harmonic signal, in contrast to (I) which does not give any noticeable signal [12].

3.3 IR and Raman spectra

The vibrational spectra of the title compounds are shown in Figs. 5 and 6, wavenumbers are collected in Table 4. The main characteristic vibrations of the spectra of (I) and (II) can be assigned based on IR and Raman spectra of aqueous solutions of L-histidine in different states of protonation [27] and vibrational spectra of L-histidine nitrates [17], and L-histidinium(+) perchlorate and L-histidinium(+) tetrafluoroborate [28].

The presence of L-histidinium(2+) cations is reflected by absorption bands at 1736 and 1727 cm^{-1} and Raman-lines at 1742 and 1729 cm^{-1}, respectively, caused by stretching vibrations of C=O bonds in the COOH groups. The respective values in the spectrum of L-$His^{2+} \cdot 2\,NO_3^-$ [17] are equal to 1729 cm^{-1} (IR) and 1735 cm^{-1} (Raman). In the region 3500−2500 cm^{-1} one can expect stretching

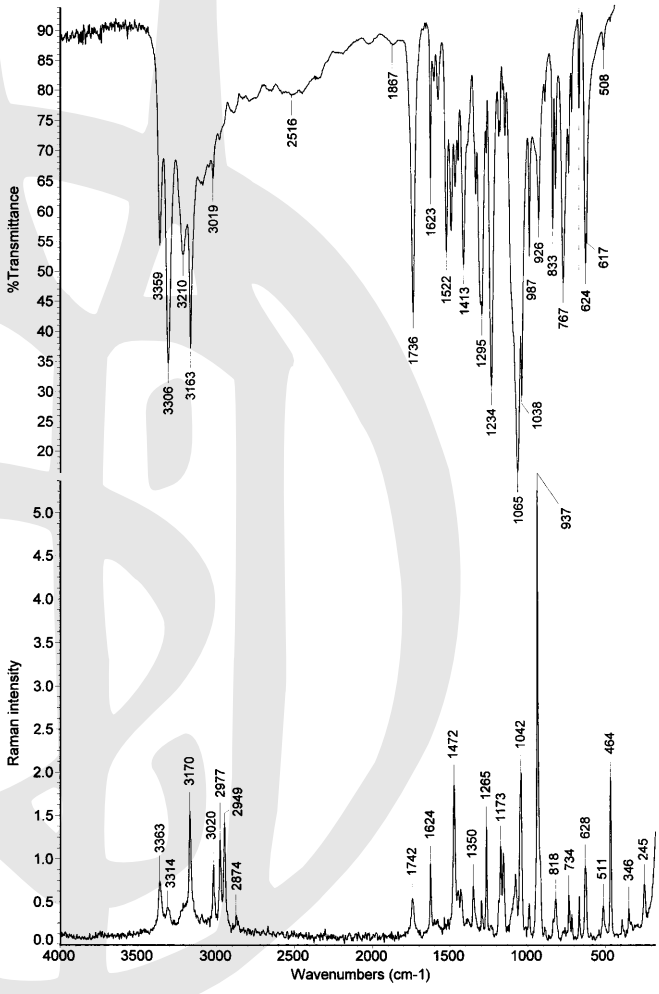

Fig. 5. IR and Raman spectra of L-$His^{2+} \cdot NO_3^- \cdot ClO_4^-$ (I).

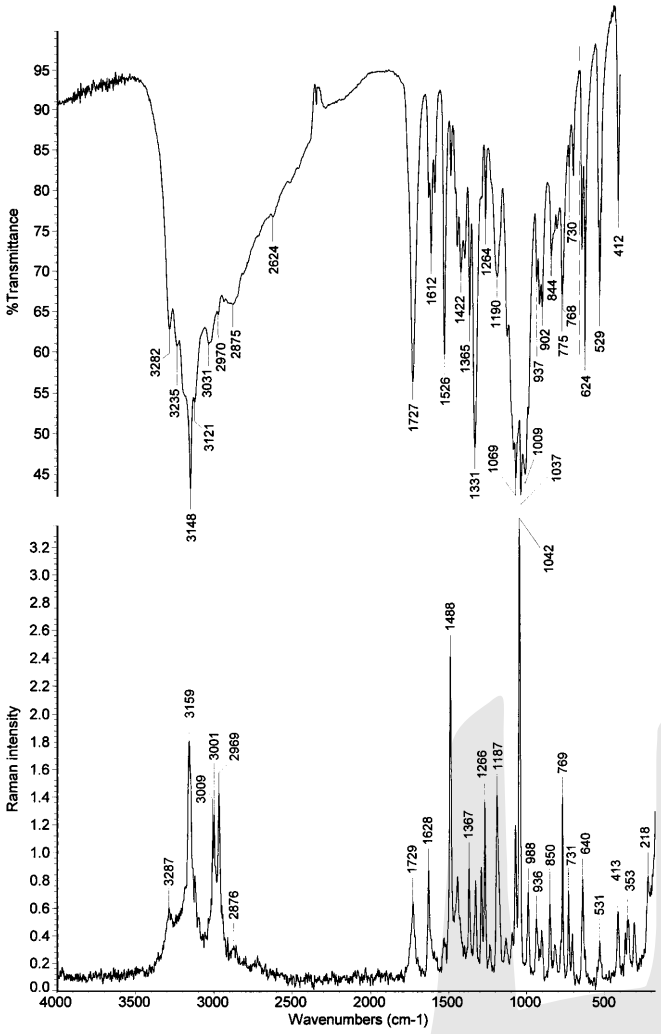

Fig. 6. IR and Raman spectra of *L*-$His^{2+} \cdot NO_3^- \cdot BF_4^-$ (II).

vibrations of C−H, N−H and O−H bonds. The characteristic stretching vibrations ν(C−H) of the imidazole ring, which are usually observed at approximately 3150(±50) cm^{-1} [1] are visible as sharp peaks at 3163 and 3148 cm^{-1} (IR) and at 3170 and 3159 cm^{-1} (Raman), respectively. The peaks at higher wavenumbers (3210, 3306, 3359 cm^{-1} for (I) and 3235, 3282 cm^{-1} for (II) and respective Raman lines) have been assigned to stretching vibrations of N−H bonds. The displacement of the (N−H) peaks towards lower frequencies in (II) corresponds to stronger hydrogen bonds compared with the hydrogen bonds in (I). Additional peaks at 3020, 2977, 2949 cm^{-1} for (I) and at 3001 and 2969 cm^{-1} for (II) as well as the respective weak bands in the IR spectrum were assigned to aliphatic CH and CH_2 groups. The O−H-stretching vibration is most probably visible in the broad band at approximately 2516 cm^{-1} due to the O···O (2.617(2) Å) hydrogen bond in (I), which usually does not appear in Raman spectra. The broadening of the band in the region near 2500 cm^{-1} (Fig. 6) may be caused by O−H-stretching vibrations in addition to more stronger N−H···O type hydrogen bonds.

The anions (NO_3^- and ClO_4^- or BF_4^-) also have characteristic peaks in the IR and/or Raman spectra. The most characteristic scattering line of the nitrate anion is the one at 1045(±10) cm^{-1} [17], caused by symmetric stretching vibration. In the Raman spectra of both title compounds, this line is visible at 1042 cm^{-1}. Respective lines in the spectra of *L*-$His^+ \cdot NO_3^- \cdot H_2O$, *L*-$His^+ \cdot NO_3^-$ and *L*-$His^{2+} \cdot 2\,NO_3^-$ appear at 1049, 1042 and 1046 cm^{-1} [17]. The symmetric stretching vibration of NO_3^- anions is often absent in the IR spectrum, since this vibration is inactive for free anions in the absorption spectrum. However, distortion of the NO_3^- anion due to hydrogen bond may lead to observation of this vibration. As was mentioned above, the bond N4−O1 is noticeably longer than two others. So bands at 1038 cm^{-1} and 1037 cm^{-1} in the IR spectra may relate to this vibration. The strong absorption bands in the spectrum of (I) at 1295 cm^{-1} and at 1331 cm^{-1} in the spectrum of (II) are probably caused by asymmetric stretching vibration of the nitrate anion. Probable assignment of deformation vibrations is indicated in Table 4.

The most characteristic vibrations of the ClO_4^- and BF_4^- anions are asymmetric stretching in the IR spectrum and symmetric stretching in the Raman spectrum. These vibrations appear in the spectra of *L*-histidinium(+) perchlorate at 1065 cm^{-1} and 930 cm^{-1}, and in those of *L*-histidinium(+) tetrafluoroborate at 1027 cm^{-1} and 770 cm^{-1} [28]. The respective vibrations can be observed also at 1065 cm^{-1} (IR) and at 937 cm^{-1} (Raman) for (I), and at 1069 cm^{-1} (IR) and at 769 cm^{-1} (Raman) for (II), although the latter is not as intensive as the one of the perchlorate anion. Assignment of deformation vibrations is indicated in Table 4.

4. Conclusion

In the present work, we have reported the preparation, crystal structure and vibrational spectra of *L*-histidinium(2+) nitrate-perchlorate and *L*-histidinium(2+) nitrate-tetrafluoroborate. Both crystals are apparently formed via a similar mechanism and exhibit similar unit cell dimensions with the same symmetry ($P2_12_12_1$). Although the packing manner of both structures is also similar, the conformations of the *L*-histidinium(2+) cations are different, which leads to different hydrogen bond networks and – more remarkable – different nonlinear optical activity. Interestingly, among the title compounds and the related salts of *L*-histidine dinitrate (*L*-$His^{2+} \cdot 2\,NO_3^-$) [18, 19], *L*-histidinium(+) nitrate monohydrate (*L*-$His^+ \cdot NO_3^- \cdot H_2O$) [17], and *L*-histidinium(+) perchlorate (*L*-$His^+ \cdot ClO_4^-$) [21], species (I) is the only one where the carbon backbone of the *L*-histidinium(2+) cation shows *gauche*-conformation. In all other cases, the conformation is *trans*.

With this contribution, we have extended the knowledge of the solid state chemistry of mixed salts of amino acids, which are not only interesting from a chemical point of view, but might also serve as a source of materials with interesting physical properties, as has been shown before for various other amino acid salts [29, 30].

Table 4. Wavenumbers and assignments in the IR and Raman spectra of the title compounds (Im – imidazole, ν – stretching, δ – deformation, ω – wagging, ϱ – rocking, sh – shoulder).

L-$His^{2+} \cdot NO_3^- \cdot ClO_4^-$ (I)		*L*-$His^{2+} \cdot NO_3^- \cdot BF_4^-$ (II)		Assignment
IR	Raman	IR	Raman	
3359	3363	3282	3287	ν(NH)
3306	3314	3235		ν(NH)
3210	3212 sh	3190 sh		ν(NH)
3163	3170	3148	3159; 3151	ν(CH) Im^+
		3121	3123 sh	ν(NH)
3084; 3045	3095			Sum tone?
3019	3020	3031	3009; 3001	ν(CH) CH
2977; 2887	2977; 2949; 2874	2970	2969	ν(CH) CH_2
2790; 2644		2934; 2875	2876	Sum tone
2516				ν(O−H)
2448				Sum tone
2186; 2019		2624		Sum tone
1867				Sum tone
1736	1742	1727	1729	ν(C=O) COOH
1623; 1600; 1574	1624; 1579	1627; 1612; 1589	1628	$\delta_{as}(NH_3^+)$; ν(C=C); ν(C=N) Im^+
1522; 1492	1512	1526	1529	$\delta_s(NH_3^+)$
1466	1472	1486; 1457	1488	$\delta(CH_2)$
1447	1447	1445	1442	
1413	1430	1422		
1387 sh	1385	1397		
1335	1350	1365	1367	ring stretching
1304; 1295	1300; 1298	1331;	1326	$\nu_{as}(NO_3^-)$
		1292 sh	1288	
1266	1265	1264	1266	ν(C−OH)
1234	1239		1235	$\omega(CH_2)$
1185	1187	1190; 1172 sh	1187	$\varrho(NH_3^+)$
1177	1173	1125; 1098 sh	1131	$\varrho(NH_3^+)$
1158; 1145	1156			$\varrho(NH_3^+)$
1093 sh; 1081 sh	1078	1085	1092	ν(C-N)
		1069	1070	$\nu_{as}(BF_4^-)$
1065				$\nu_{as}(ClO_4^-)$
	1042		1042	$\nu_s(NO_3^-)$
1038		1037		$\nu_s(NO_3^-)$?
987	990	1009		
	937			$\nu_s(ClO_4^-)$
926	919 sh	937; 919; 902	936;903	
884	890	844	850	
833; 816	835 sh; 818	827 sh; 808	822	$\delta_s(NO_3^-)$
767	771; 760	775; 768		
			769	$\nu_s(BF_4^-)$
731	734			
712	715	730	731	$\delta_{as}(NO_3^-)$
665	667	703	707	ring deformation
		664	640	
624;617	628			$\delta_{as}(ClO_4^-)$
		624	626 sh	
508	511			
		536; 529; 519	531	$\delta_{as}(BF_4^-)$
	464			$\delta_s(ClO_4^-)$
464	390	412	413; 367	
			353	$\delta_s(BF_4^-)$
	346; 245		346; 309; 218	

Acknowledgments. The present research has been carried out in frame of Project #0111 supported by the Government of Armenia and ANSEF (PS1839 Project). The authors thank R.A. Apreyan and G.G. Martirosyan for their help.

References

[1] Petrosyan, A. M.: Salts of L-histidine As Nonlinear Optical Materials: A Review. J. Crystallization Physics and Chemistry **1(1)** (2010) 33–56.

[2] Fleck, M.: Compounds of glycine with halogen or metal halogenides: review and comparison. Z. Kristallogr. **223** (2008) 222–232.

[3] Petrosyan, A. M.: Formation mechanisms of nonlinear optical crystalline salts of L-arginine and L-histidine. Proc. Conf. "Laser Physics-2003", Oct. 14–17, 2003, Ashtarak, Armenia, 2004, 148–151.

[4] Vilminot, S.; Cot, L.: Sur deux nouveaux sulfates de glycine et d'ion monovalent. C. R. Acad. Sci. Paris, Ser. C t. **277** (1973) 1355–1358.

[5] Vilminot, S.; Philippot, E.; Cot, L.: Structure du sulfate d'ammonium et de glycinium $NH_4NH_3CH_2COOHSO_4$. Acta Crystallogr. B**30** (1974) 2602–2606.

[6] Vilminot, S.; Philippot, E.; Lehmann, M.: Affinement de la structure de $NH_4NH_3CH_2COOHSO_4$ par diffraction neutronique. Acta Crystallogr. B**32** (1976) 1817–1822.

[7] Haussühl, S.; Schreuer, J.: Crystal structure, thermal expansion and elastic properties of triclinic betaine hydrogen ammonium sulfate $((CH_3)_3NCH_2COOH)NH_4SO_4$. Z. Kristallogr. **211** (1996) 79–83.

[8] Saari, A. L.; Anderson, R. H.: Amino acid derivatives. US Patent 4064138, 1977.

[9] Srinivasan, N.; Sridhar, B.; Rajaram, R. K.: Hydrogen bis[*L*-lysinium(2+)] dichloride perchlorate. Acta Crystallogr. E**57** (2001) o875–o877.

[10] Srinivasan, N.; Sridhar, B.; Rajaram, R. K.: *L*-Lysine *L*-Lysinium dichloride nitrate. Acta Crystallogr. E 57 (2001) o888–o890.

[11] Ramaswamy, S.; Sridhar, B.; Ramakrishnan, V.; Rajaram, R. K.: Bis(*L*-ornithinium) chloride nitrate sulfate. Acta Crystallogr. E**60** (2004) o768–o770.

[12] Petrosyan, A. M.; Karapetyan, H. A.; Ghazaryan, V. V.: New approach for searching nonlinear optical materials among salts of amino acids. Proc. conf. "Laser Physics-2008" 14–17 Oct. 2008, Ashtarak, Armenia 2009, 63–66.

[13] Ravi, G.; Srinivasan, K.; Anbukumar, S.; Ramasamy, P.: Growth and characterization of sulphate mixed L-arginine phosphate and ammonium dihydrogen phosphate/potassium dihydrogen phosphate mixed crystals. J. Crystal Growth **137** (1994) 598–604.

[14] Pal, T.; Kar, T.; Wang, X.-Q.; Zhou, G.-Y.; Wang, D.; Cheng, X.-F.; Yang, Z.-H.: Growth and characterization of nonlinear optical material, LAHClBr – a new member of L-arginine halide family. J. Crystal Growth **235** (2002) 523–528.

[15] Mallik, T.; Kar, T.: Crystallization and characterization of nonlinear optical material L-arginine formomaleate. Mater. Lett. **61** (2007) 3826–3828.

[16] Marcy, H. O.; Rosker, M. J.; Warren, L. F.; Cunningham, P. H.; Thomas, C. A.; Deloach, L. A.; Velesko, S. P.; Ebbers, C. A.; Liao, J.-H.; Kanatzidis, M. G.: L-Histidine tetrafluoroborate a solution-grown semiorganic crystal for nonlinear frequency conversion. Optics Letters **20** (1995) 252–254.

[17] Petrosyan, H. A.; Karapetyan, H. A.; Petrosyan, A. M.: L-histidine nitrates. J. Molec. Structure **794** (2006) 160–167.

[18] Bahadur, S. A.: Crystal structure analyses of aminoacid inorganic complexes. PhD Thesis, Madurai Kamaraj University, Madurai, India, 1992.

[19] Benali-cherif, N.; Benguedouar, L.; Cherouana, A.; Bendjeddou, L.; Merazig, H.: L-Histidinium dinitrate. Acta Crystallogr. E **58** (2002) o822–o824.

[20] Aruna, S.; Bhagavannarayana, G.; Sagayaraj, P.: Investigation on the physicochemical properties of nonlinear optical (NLO) single crystal: *L*-histidinium dinitrate. J. Crystal Growth **304** (2007) 184–190.

[21] Román, P.; Gutiérrez-Zorrilla, J. M.; Luque, A.; Vegas, A.: The MoO_3-histidine-$HClO_4$ system. Synthesis, spectroscopic, and structural study of *L*-histidinium perchlorate. J. Crystallogr. Spectrosc. Res. **17** (1987) 585–595.

[22] Otwinowski, Z.; Minor, W.: Processing of X-ray Diffraction Data Collection in Oscillation Mode. Methods Enzymol., part A **276** (1997) 307–326.

[23] Sheldrick, G. M.: A short history of SHELX. Acta Crystallogr. A **64** (2008) 112–122.

[24] Flack, H. D.: On enantiomorph-polarity estimation. Acta Crystallogr. A **39** (1983) 876–881.

[25] Zefirov, Yu. V.: Crystallographic angle criteria of intermolecular hydrogen bonds. Kristallografia **44** (1999) 1091–1093.

[26] Gokul Raj, S.; Ramesh Kumar, G.; Mohan, R.; Jayavel, R.; Varghese, B.: Crystal structure and vibrational analysis of novel nonlinear optical L-histidinium tetrafluoroborate (L-HFB) single crystals. Phys. St. Sol. (b) **244** (2007) 558–568.

[27] Mesu, J. G.; Visser, T.; Soulimani, F.; Weckhuysen, B. M.: Infrared and Raman spectroscopic study of pH-induced structural changes of *L*-histidine in aqueous environment. Vibrational Spectroscopy **39** (2005) 114–125.

[28] Petrosyan, A. M.: Vibrational spectra of *L*-histidine perchlorate and *L*-histidine tetrafluoroborate. Vibrational Spectroscopy **43** (2007) 284–289.

[29] Kaminskii, A. A.; Bohatý, L.; Becker, P.; Held, P.; Eichler, H. J.; Rhee, H.; Hanuza, J.: Orthorhombic tris(glycine) zinc chloride Gly_3ZnCl_2 – a new semi-organic many-phonon SRS crystal manifesting different nonlinear-laser ($\chi(3) \leftrightarrow \chi(2)$) interactions under one-micron picosecond pumping. Laser Phys. Lett. **6** (2009) 872–885.

[30] Fleck, M.; Becker, P.; Bayarjargal, L.; Ochrombel, R.; Bohatý, L.: Crystal growth, crystal structure and physical properties of polar orthorhombic tris(glycine) zinc chloride. Cryst. Res. Technol. **43** (2008) 127–134.